

In-Medium Pion Valence Distributions in a Light-Front Model

J. P. B. C de Melo^a, K. Tsushima^a, and I. Ahmed^{a,b}

^a*Laboratório de Física Teórica e Computacional - LFTC, Universidade Cruzeiro do Sul, 01506-000 São Paulo, Brazil*

^b*National Center for Physics, Quaid-i-Azam University Campus, Islambad 45320, Pakistan*

Abstract

Pion valence distributions in nuclear medium and vacuum are studied in a light-front constituent quark model. The in-medium input for studying the pion properties is calculated by the quark-meson coupling model. We find that the in-medium pion valence distribution, as well as the in-medium pion valence wave function, are substantially modified at normal nuclear matter density, due to the reduction in the pion decay constant.

Key words: Pion, Nuclear Medium, Light-Front, Pion Distribution Amplitude, Parton Distribution

Introduction: One of the most exciting and challenging topics in hadronic and nuclear physics is to study the modifications of hadron properties in nuclear medium (nuclear environment), and also how such modifications affect the observables differently from those in vacuum. Since hadrons are composed of quarks, antiquarks and gluons, it is natural to expect that hadron internal structure would change when they are immersed in nuclear medium or in atomic nuclei [1,2,3,4,5]. This question, to study the medium modification of hadron internal structure, is particularly interesting when it comes to that of pion. To be able to study the properties of pion in nuclear medium, one first needs, simpler, effective quark-antiquark models of pion, which are successful in describing its properties in vacuum. Among such models, light-front constituent quark model has been very successful in describing the hadronic properties in vacuum, in particular, the electromagnetic form factors, electromagnetic radii and decay constants of pion and kaon [6,7,8,9,10,11,12]. Recent advances in experiments, indeed suggest to make it possible to access to the pion (hadronic) properties in a nuclear medium [3,4,5,13,14].

Among the all hadrons, pion is the lightest, and it is believed as a Nambu-Goldstone boson, which is realized in nature emerged by the spontaneous breaking of chiral symmetry. This Nambu-Goldstone boson, pion, plays very important and special roles in hadronic and nuclear physics [15,16,17,18,19,20,21,22,23,24,25,26]. However, because of its special properties, particularly the unusually light mass, it is not easy to describe the pion properties in medium as well as in vacuum based on naive quark models, even though such models can be successful in describing the other hadrons.

Despite of this difficulty, some important studies were made [27,28,29] on the pion structure and its role in a nuclear medium. Recently, we also studied the properties of pion in nuclear medium [13,14], namely, the electromagnetic form factor, charge radius and weak decay constant, by using a light-front constituent quark model. There, the in-medium input was calculated by the quark-meson coupling (QMC) model [3,30]. We have predicted the in-medium changes of pion properties [13,14]: (i) faster falloff of the pion charge form factor as increasing the negative of the four-momentum transfer squared, (ii) increasing of the root mean-square charge radius as increasing nuclear density, and (iii) decreasing of the decay constant as increasing nuclear density. The purpose of this work is, to extend our work for the pion in medium made in Refs. [13,14], and study the pion valence distribution amplitude in symmetric nuclear matter. We find substantial modification of the pion valence wave function and distribution amplitude in symmetric nuclear matter at normal nuclear matter density.

The QMC Model: First, we briefly review the QMC model, the quark-based model of nuclear matter, to study the pion properties in medium. The effective Lagrangian density for a uniform, spin-saturated, and isospin-symmetric nuclear system (symmetric nuclear matter) at the hadronic level is given by [30,31],

$$\mathcal{L} = \bar{\psi}[i\gamma \cdot \partial - m_N^*(\hat{\sigma}) - g_\omega \hat{\omega}^\mu \gamma_\mu]\psi + \mathcal{L}_{\text{meson}} , \quad (1)$$

where ψ , $\hat{\sigma}$ and $\hat{\omega}$ are respectively the nucleon, Lorentz-scalar-isoscalar σ , and Lorentz-vector-isoscalar ω field operators with,

$$m_N^*(\hat{\sigma}) \equiv m_N - g_\sigma(\hat{\sigma})\hat{\sigma}. \quad (2)$$

Note that, in symmetric nuclear matter isospin-dependent ρ -meson mean field is zero, and thus we have omitted it. Then the relevant free meson Lagrangian density is given by,

$$\mathcal{L}_{\text{meson}} = \frac{1}{2}(\partial_\mu \hat{\sigma} \partial^\mu \hat{\sigma} - m_\sigma^2 \hat{\sigma}^2) - \frac{1}{2} \partial_\mu \hat{\omega}_\nu (\partial^\mu \hat{\omega}^\nu - \partial^\nu \hat{\omega}^\mu) + \frac{1}{2} m_\omega^2 \hat{\omega}^\mu \hat{\omega}_\mu. \quad (3)$$

Hereafter, we consider the symmetric nuclear matter at rest. Then, within Hartree mean-field approximation, the nuclear (baryon) and scalar densities are respectively given by,

$$\begin{aligned}\rho &= \frac{4}{(2\pi)^3} \int d\vec{k} \theta(k_F - |\vec{k}|) = \frac{2k_F^3}{3\pi^2}, \\ \rho_s &= \frac{4}{(2\pi)^3} \int d\vec{k} \theta(k_F - |\vec{k}|) \frac{m_N^*(\sigma)}{\sqrt{m_N^{*2}(\sigma) + \vec{k}^2}},\end{aligned}\quad (4)$$

here, $m_N^*(\sigma)$ is the value (constant) of effective nucleon mass at given density (see also Eq. (2)). In the standard QMC model [3,30,31] the MIT bag model is used, and the Dirac equations for the light quarks inside a nucleon (bag) composing nuclear matter, are given by,

$$\left[i\gamma \cdot \partial_x - (m_q - V_\sigma^q) \mp \gamma^0 \left(V_\omega^q + \frac{1}{2} V_\rho^q \right) \right] \begin{pmatrix} \psi_u(x) \\ \psi_{\bar{u}}(x) \end{pmatrix} = 0, \quad (5)$$

$$\left[i\gamma \cdot \partial_x - (m_q - V_\sigma^q) \mp \gamma^0 \left(V_\omega^q - \frac{1}{2} V_\rho^q \right) \right] \begin{pmatrix} \psi_d(x) \\ \psi_{\bar{d}}(x) \end{pmatrix} = 0. \quad (6)$$

Because the nuclear matter interactions are strong interactions, the Coulomb interaction is neglected as usual, and SU(2) symmetry is assumed, $m_{u,\bar{u}} = m_{d,\bar{d}} \equiv m_{q,\bar{q}}$. The corresponding effective (constituent) quark masses are defined by, $m_{u,\bar{u}}^* = m_{d,\bar{d}}^* = m_{q,\bar{q}}^* \equiv m_{q,\bar{q}} - V_\sigma^q$, to be explained later.

As mentioned already, in symmetric nuclear matter within Hartree approximation, the ρ -meson mean field is zero, $V_\rho^q = 0$, in Eq. (6), and we ignore it. The constant mean-field potentials are defined as, $V_\sigma^q \equiv g_\sigma^q \sigma = g_\sigma^q \langle \sigma \rangle$, and, $V_\omega^q \equiv g_\omega^q \omega = g_\omega^q \langle \omega \rangle$, with g_σ^q , and g_ω^q , are the corresponding quark-meson coupling constants, where the quantities with the brackets stand for the expected values in symmetric nuclear matter [3]. Since the average velocity is zero, $\langle \bar{\psi}_q \vec{\gamma} \psi_q \rangle = 0$, in the nuclear matter rest frame, no spacial-dependent source for the vector-meson mean fields arise, and only the terms proportional to γ^0 are kept in Eq. (6). (More details are given in Ref. [3].)

The same meson mean fields σ and ω for the quarks in Eqs. (5) and (6), satisfy self-consistently the following equations at the nucleon level:

$$\omega = \frac{g_\omega \rho}{m_\omega^2}, \quad (7)$$

$$\sigma = \frac{g_\sigma}{m_\sigma^2} C_N(\sigma) \frac{4}{(2\pi)^3} \int d\vec{k} \theta(k_F - |\vec{k}|) \frac{m_N^*(\sigma)}{\sqrt{m_N^{*2}(\sigma) + \vec{k}^2}} = \frac{g_\sigma}{m_\sigma^2} C_N(\sigma) \rho_s, \quad (8)$$

$$C_N(\sigma) = \frac{-1}{g_\sigma(\sigma=0)} \left[\frac{\partial m_N^*(\sigma)}{\partial \sigma} \right], \quad (9)$$

where $C_N(\sigma)$ is the constant value of the scalar density ratio [3,30,31]. Because

Table 1

Coupling constants, and calculated properties for symmetric nuclear matter at normal nuclear matter density $\rho_0 = 0.15 \text{ fm}^{-3}$, for $m_q = 5$ and 220 MeV (the latter values is used in this study and was used in Refs. [12,13]). The effective nucleon mass, m_N^* , and the nuclear incompressibility, K , are quoted in MeV. (See Ref. [3] for details.)

$m_q(\text{MeV})$	$g_\sigma^2/4\pi$	$g_\omega^2/4\pi$	m_N^*	K
5	5.39	5.30	754.6	279.3
220	6.40	7.57	698.6	320.9

of the underlying quark structure of the nucleon used to calculate $M_N^*(\sigma)$ in nuclear medium (see Eq. (2)), $C_N(\sigma)$ gets nonlinear σ -dependence, whereas the usual point-like nucleon-based model yields unity, $C_N(\sigma) = 1$.

It is this $C_N(\sigma)$ or $g_\sigma(\sigma)$ that gives a novel saturation mechanism in the QMC model, and contains the important dynamics which originates in the quark structure of the nucleon. Without an explicit introduction of the nonlinear couplings of the meson fields in the Lagrangian density at the nucleon and meson level, the standard QMC model yields the nuclear incompressibility of $K \simeq 280$ MeV with $m_q = 5$ MeV, which is in contrast to a naive version of quantum hadrodynamics (QHD) [32] (the point-like nucleon model of nuclear matter), results in the much larger value, $K \simeq 500$ MeV; the empirically extracted value falls in the range $K = 200 - 300$ MeV. (See Ref. [33] for the updated discussions on the incompressibility.)

Once the self-consistency equation for the σ including the quark Dirac equations, Eqs. (5), (6), and Eq. (8) have been solved, one can evaluate the total energy per nucleon:

$$E^{\text{tot}}/A = \frac{4}{(2\pi)^3\rho} \int d\vec{k} \theta(k_F - |\vec{k}|) \sqrt{m_N^{*2}(\sigma) + \vec{k}^2} + \frac{m_\sigma^2\sigma^2}{2\rho} + \frac{g_\omega^2\rho}{2m_\omega^2}. \quad (10)$$

We then determine the coupling constants, g_σ and g_ω , so as to fit the binding energy of 15.7 MeV at the saturation density $\rho_0 = 0.15 \text{ fm}^{-3}$ ($k_F^0 = 1.305 \text{ fm}^{-1}$) for symmetric nuclear matter.

In Refs. [12,13], the quark mass in vacuum was used $m_{q,\bar{q}} = 220$ MeV to study the pion properties in symmetric nuclear matter. With this value the model can reproduce the electromagnetic form factor and the decay constant well in vacuum [8]. Thus, we use the same value in this study. The corresponding coupling constants and some calculated properties for symmetric nuclear matter at the saturation density ρ_0 , with the standard values of $m_\sigma = 550$ MeV and $m_\omega = 783$ MeV, are listed in Table 1. For comparison, we also give the cor-

responding quantities calculated in the standard QMC model with a vacuum quark mass of $m_q = 5$ MeV (see Ref. [3] for details). Thus we have obtained the necessary properties of the light-flavor constituent quarks in symmetric nuclear matter with the empirically accepted data for a vacuum constituent light-quark mass of $m_q = 220$ MeV; namely, the density dependence of the effective mass (scalar potential) and vector potential. The same in-medium constituent quark properties which reproduce the nuclear saturation properties (and used in Refs. [13,14]) will be used as input to study the pion properties in symmetric nuclear matter.

In Figs. 1 and 2 we respectively show our results for the negative of the binding energy per nucleon ($E^{\text{tot}}/A - m_N$), effective constituent light-quark mass, m_q^* , in symmetric nuclear matter (left panel of Fig. 2), and the in-medium pion decay constant, f_π^* (right panel of Fig. 2), which were calculated in Ref. [12,13]. For f_π^* shown in the right panel of Fig. 2, more explanations will be given later. Thus, we can say that the in-medium pion properties (f_π^* as well), are driven by the effective constituent light-quark mass m_q^* , which is self-consistently calculated and constrained by the symmetric nuclear matter saturation properties.

Next, we study the pion valence wave function and distribution amplitude (DA) in symmetric nuclear matter using the in-medium constituent light-quark properties obtained so far.

The Model: The light-front constituent quark model we use here [8,9], although simple, is quite successful in describing the properties of pion in vacuum, such as the electromagnetic form factor, charge radius and weak decay constant. The model was also extended for kaon in Ref. [11]. This fact of success in describing properties in vacuum is a prerequisite to study the in-medium changes of the pion and kaon properties. In this study, we focus on the pion. For some in-medium properties of pion studied in the past, see Ref. [13]. Note that, we simply use the terminology *medium* or *nuclear medium* hereafter, instead of explicitly specifying *symmetric nuclear matter*, otherwise stated.

To study the in-medium pion properties, we use the input calculated by the quark-meson coupling (QMC) model [3] as mentioned already. The QMC model was invented by Guichon [30] to describe the nuclear matter based on the quark degrees of freedom. The self-consistent exchange of the scalar-isoscalar σ and vector-isoscalar ω mean fields coupled directly to the relativistic confined quarks, are the key and novelty for the new saturation mechanism of nuclear matter as we explained. The model was extended, and has successfully been applied for various nuclear and hadronic phenomena [3]. In the following we briefly summarize the input used for the present study of the pion properties in nuclear medium.

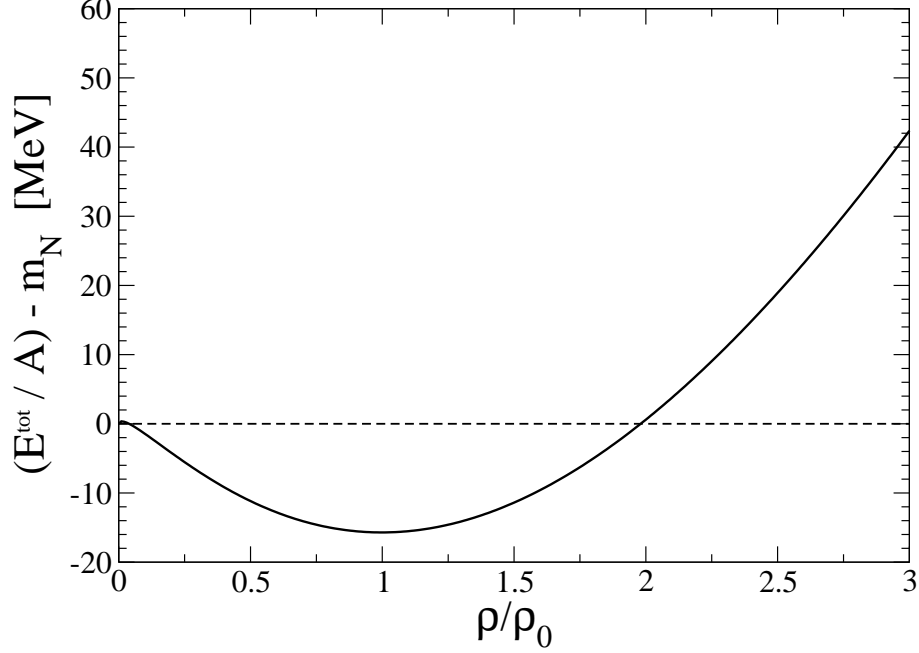


Fig. 1. Negative of the binding energy per nucleon for symmetric nuclear matter, $(E^{tot}/A) - m_N$, as a function of nuclear density ρ ($\rho_0 = 0.15 \text{ fm}^{-3}$) with the vacuum quark mass value $m_q = m_{\bar{q}} = 220 \text{ MeV}$ ($q = u, d$), calculated by the QMC model (taken from Ref. [13]). The corresponding incompressibility K obtained is $K = 320.9$

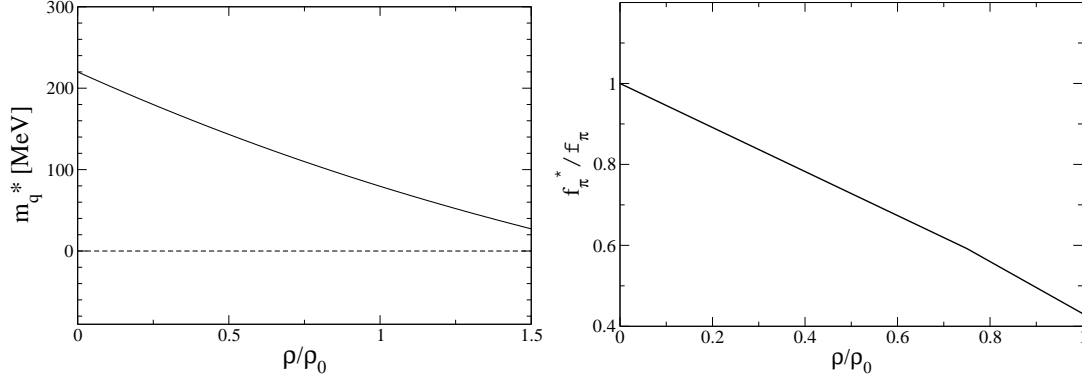


Fig. 2. Effective constituent quark mass m_q^* ($q = \bar{q} = u, \bar{u}, d, \bar{d}$) (left panel), and the pion decay constant calculated in symmetric nuclear matter (right panel), both taken from Ref. [13].

The constituent mass of the light quarks (q and \bar{q} , with $q = u, d$) in the light-front constituent quark model in vacuum [13] is, $m_q = m_{\bar{q}} = 220 \text{ MeV}$. Then, all the nuclear matter saturation properties are generated by using this light-quark mass value. In other words, the different values of m_q in vacuum generate the corresponding different nuclear matter properties, except for the saturation point of the symmetric nuclear matter, $\rho = \rho_0$ (normal nuclear matter density, 0.15 fm^{-3}) with the empirically extracted binding energy of 15.7 MeV . This saturation point condition is generally used to constrain the

models of nuclear matter.

Here, we note that the pion mass up to normal nuclear matter density is expected to be modified only slightly, where the modification δm_π at nuclear density $\rho = 0.17 \text{ fm}^{-3}$, averaged over the pion isospin states, is estimated as $\delta m_\pi \simeq +3 \text{ MeV}$ [4,34,35,36]. Therefore, we approximate the effective pion mass value in nuclear medium to be the same as in vacuum, $m_\pi^* = m_\pi$, up to $\rho = \rho_0 = 0.15 \text{ fm}^{-3}$, the maximum nuclear matter density treated in this study. Furthermore, since the light-front constituent quark model is rather simple, and based on a naive constituent quark picture, the model cannot discuss the chiral limit of vanishing (effective) light-quark masses.

We next study the pion properties in symmetric nuclear matter. The effective interaction Lagrangian density for the quarks and pion in medium is given by,

$$\mathcal{L}_{\text{eff}} = -ig^* (\bar{q}\gamma^5 \vec{\tau} q \cdot \vec{\phi}) \Lambda^* , \quad (11)$$

where the coupling constant, $g^* = m_q^*/f_\pi^*$, is obtained by the "in-medium Goldberger-Treiman relation" at the quark level, with m_q^* and f_π^* being respectively the effective constituent quark mass and pion decay constant in medium, $\vec{\phi}$ the pion field [8,9,11], and Λ^* is the π - q - \bar{q} vertex function in medium. Hereafter, the in-medium quantities are indicated with the asterisk, *.

Symmetric pion valence wave function: The pion valence wave function used in this study to calculate the pion distribution amplitude (poion DA) [37,38], (and to be able to calculate also parton distribution function [39,40]), is symmetric under the exchange of quark and antiquark momenta. This π - q - \bar{q} vertex function, $\Lambda(k, P)$ in vacuum with the arguments k and P stand for momenta, is the same as that used for studying the properties of pion [8,9,41] and kaon [11]. However, for the in-medium Λ^* , the arguments of the function are replaced by those of the in-medium [13]:

$$\Lambda^*(k + V, P) = \frac{C^*}{((k + V)^2 - m_R^2 + i\epsilon)} + \frac{C^*}{((P - k - V)^2 - m_R^2 + i\epsilon)}, \quad (12)$$

where $V^\mu = \delta_0^\mu V^0$ is the vector potential felt by the light quarks in the pion immersed in medium, and can be eliminated by the variable change in the k -integration, $k^\mu + \delta_0^\mu V^0 \rightarrow k^\mu$. The normalization factor associated with C^* is modified by the medium effects. (See also below Eq. (14), and Ref. [13] for details.) The regulator mass m_R represents soft effects at short range of about the 1 GeV scale, and m_R may also be influenced by in-medium effects. However, we employ $m_R^* = m_R$ in Eq. (12), since there exists no established way of estimating this effect on the regulator mass. This can avoid introducing extra source of uncertainty.

The Bethe-Salpeter amplitude in medium, Ψ_π^* , with the vertex function in

medium Λ^* is given by,

$$\Psi_\pi^*(k+V, P) = \frac{\not{k} + \not{V} + m_q^*}{(k+V)^2 - m_q^{*2} + i\epsilon} \gamma^5 \Lambda^*(k+V, P) \times \frac{\not{k} + \not{V} - \not{P} + m_q^*}{(k+V-P)^2 - m_q^{*2} + i\epsilon}. \quad (13)$$

By eliminating the instantaneous terms, namely eliminating the terms with gamma matrix γ^+ in the numerators and k^+ and $(P^+ - k^+)$ in the denominators with the light-front convention $a^\pm \equiv a^0 \pm a^3$, and integrating over the light-front energy k^- , we obtain the in-medium pion valence wave function Φ_π^* ,

$$\Phi_\pi^*(k^+, \vec{k}_\perp; P^+, \vec{P}_\perp) = \frac{P^+}{m_\pi^{*2} - M_0^2} \left[\frac{N^*}{(1-x)(m_\pi^{*2} - \mathcal{M}^2(m_q^{*2}, m_R^2))} + \frac{N^*}{x(m_\pi^{*2} - \mathcal{M}^2(m_R^2, m_q^{*2}))} \right], \quad (14)$$

where, $N^* = C^*(m_q^*/f_\pi^*)(N_c)^{\frac{1}{2}}$ is the normalization factor with the number of colors N_c [8,9,13], $x = k^+/P^+$ with $0 \leq x \leq 1$, $\mathcal{M}^2(m_a^2, m_b^2) \equiv \frac{\vec{k}_\perp^2 + m_a^2}{x} + \frac{(\vec{P}-\vec{k})_\perp^2 + m_b^2}{1-x} - \vec{P}_\perp^2$, the square of the mass M_0^2 is $M_0^2 = \mathcal{M}^2(m_q^{*2}, m_q^{*2})$, and m_R is the regulator mass with the value $m_R^* = m_R = 600$ MeV [8,13]. Note that the model used in Refs. [7,10] does not have the second term in Eq. (14). This means that the pion valence wave function in Refs. [7,10] is not symmetric under the exchange of quark and antiquark momenta.

The present model with the symmetric vertex [8,9,11,41], was demonstrated successful in describing the pion properties in nuclear medium [13,14]. The pion transverse momentum probability density in medium, $P_\pi^*(k_\perp)$, in the pion rest frame $P^+ = m_\pi^*$ is calculated by,

$$P_\pi^*(k_\perp) = \frac{1}{4\pi^3 m_\pi^*} \int_0^{2\pi} d\phi \int_0^{m_\pi^*} \frac{dk^+ M_0^{*2}}{k^+(m_\pi^* - k^+)} |\Phi_\pi^*(k^+, \vec{k}_\perp; m_\pi^*, \vec{0})|^2, \quad (15)$$

and the integration over k_\perp for $P_\pi^*(k_\perp)$ leads to the in-medium probability of the valence component in the pion, η^* [8,9,13]:

$$\eta^* = \int_0^\infty dk_\perp k_\perp P_\pi^*(k_\perp). \quad (16)$$

The pion decay constant in medium (see Fig. 2 (right panel)), in terms of the pion valence component with $\Phi_\pi^*(k^+, \vec{k}_\perp; m_\pi^*, \vec{0})$, is calculate by [8,13]:

Table 2

Properties of pion in medium, taken from Ref. [13], with $\rho_0 = 0.15 \text{ fm}^{-3}$.

ρ/ρ_0	m_q^* [MeV]	f_π^* [MeV]	$\langle r_\pi^{*2} \rangle^{1/2}$ [fm]	η^*
0.00	220	93.1	0.73	0.782
0.25	179.9	80.6	0.84	0.812
0.50	143.2	68.0	1.00	0.843
0.75	109.8	55.1	1.26	0.878
1.00	79.5	40.2	1.96	0.930

$$f_\pi^* = \frac{m_q^*(N_c)^{1/2}}{4\pi^3} \int \frac{d^2k_\perp dk^+}{k^+(m_\pi^* - k^+)} \Phi_\pi^*(k^+, \vec{k}_\perp; m_\pi^*, \vec{0}). \quad (17)$$

Some properties of the pion in symmetric nuclear matter obtained in Ref. [13], are summarized in table 2. The results listed in table 2 are summarized as follows. As the nuclear density increases, the in-medium effective constituent quark mass, m_q^* , and the pion decay constant, f_π^* , decrease, while the root mean square charge radius, $\langle r_\pi^{*2} \rangle^{1/2}$, and the probability of valence component in the pion state, η^* , increase. This can be understood as follows. The reduction in mass, m_q^* , makes it easier to excite the valence quark component in the pion, and resulting to increase the valence component probability η^* in the pion. Furthermore, the valence wave function spreads more in coordinate space by the decrease of m_q^* , and reduces the absolute value of the wave function at the origin ($f_\pi^* \propto |\Phi_\pi^*(\vec{r} = \vec{0})|$ reduction [42]), namely, increases $\langle r_\pi^{*2} \rangle^{1/2}$.

In-medium pion Distribution Amplitude: Pion DA provides information on the nonperturbative regime of the bound state nature of pion due to the quark and antiquark at higher momentum transfer, and it was calculated with different approaches, such as QCD sum rules [43,44], and lattice QCD [45]. Our study here is based on the light-front constituent quark model.

The pion valence wave function in vacuum is normalized by [46,47] (aside from the factor $\sqrt{2}$ difference):

$$\int_0^1 dx \int \frac{d^2k_\perp}{16\pi^3} \Phi_\pi(x, \vec{k}_\perp) = \frac{f_\pi}{2\sqrt{6}}. \quad (18)$$

This is an important constraint on the normalization of the $q\bar{q}$ wave function [46,47], associated with a probability of finding a pure $q\bar{q}$ state in the pion state. According to this normalization, the in-medium pion valence wave

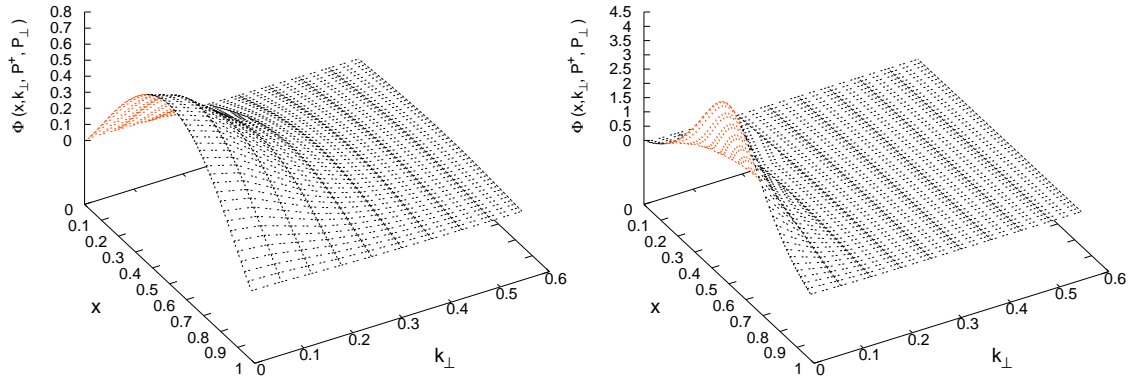


Fig. 3. Pion valence wave functions in vacuum ($\rho = 0$) [left panel] and in medium ($\rho = \rho_0$) [right panel] v.s. x and $k_\perp = |\vec{k}_\perp|$, where $P^+ = m_\pi = m_\pi^*$ and $P_\perp = |\vec{P}_\perp| = 0$. The wave functions are given in the units, $10^{-8} \times (\text{GeV})^{-1}$. Notice that the differences in the vertical axis scales for the left and right panels.

function is normalized by replacing $f_\pi \rightarrow f_\pi^*$ in the above. Since the pion decay constant in nuclear medium is modified, the pion valence wave function in nuclear medium is also modified via this normalization.

In order to examine more in detail as to how the change in f_π^* impacts on the in-medium pion valence wave function, we show in Fig. 3 the pion valence wave functions in vacuum (left panel) and $\rho = \rho_0$ (right panel).

One can notice that the in-medium pion valence wave function in momentum space has a sharper peak and localized in narrower regions both in x and k_\perp than those in vacuum. Of course, the total volume, the quantity integrated over x and \vec{k}_\perp , is reduced in medium, corresponding to the reduced f_π^* . This fact is reflected in the wave function in coordinate space, that it becomes spread wider, and generally its height is reduced.

The corresponding pion valence DA in medium, denoted by $\phi_{DA}^*(x)$ (not normalized to unity), is calculated as

$$\phi_{DA}^*(x) = \int \frac{d^2 k_\perp}{16\pi^3} \Phi_\pi^*(x, \vec{k}_\perp). \quad (19)$$

Note that, Eq. (19) holds also for the other pseudoscalar mesons M_{ps} such as kaon and D-meson, by replacing $\Phi_\pi^*(x, \vec{k}_\perp) \rightarrow \Phi_{M_{ps}}^*(x, \vec{k}_\perp)$ in the above.

We show in Fig. 4 the pion valence DA, $\phi_{DA}^*(x)$, for several nuclear densities in-

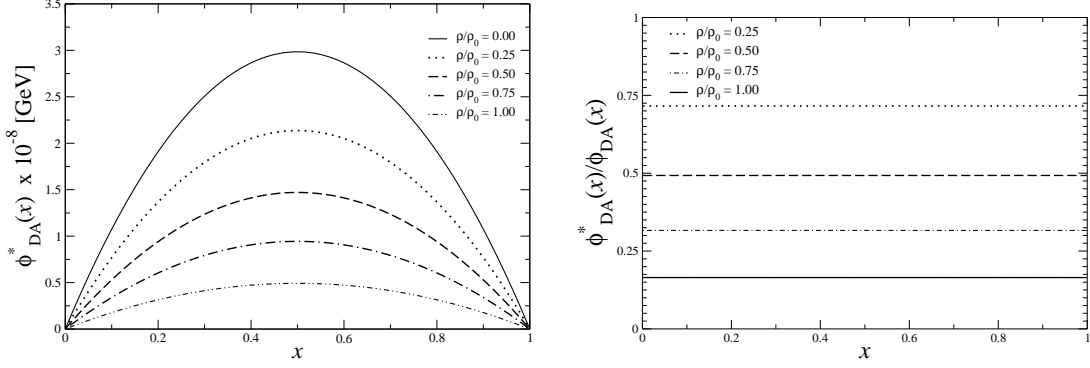


Fig. 4. Pion valence distribution amplitudes (left panel), and the ratios divided by that of the vacuum (right panel). (See also table. 2.)

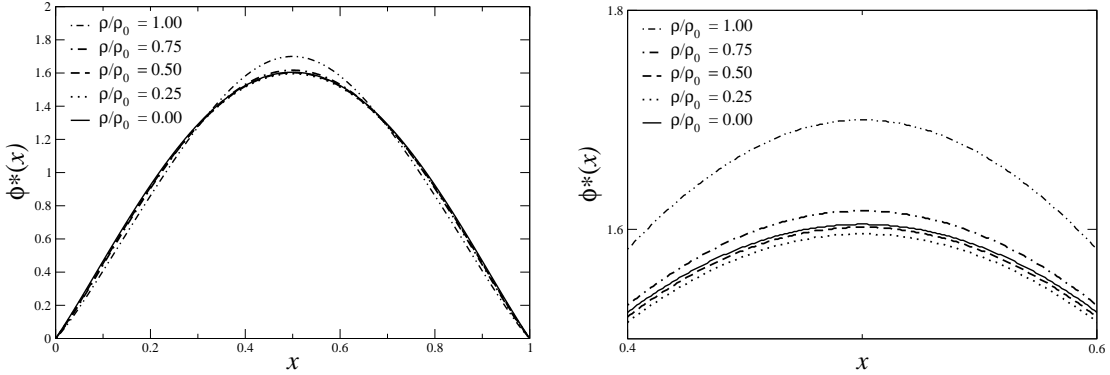


Fig. 5. Normalized pion valence distribution amplitudes (left panel), and the magnified ones (right panel), both in vacuum and in medium.

cluding in vacuum $\rho/\rho_0 = 0$ (left panel), and the corresponding ratios divided by the vacuum one $\phi_{DA}(x)$ (right panel). Indeed, the significant reduction of the in-medium pion valence DAs ($\phi_{DA}^*(x)$) is obvious in Fig. 4, reflecting the reduction of f_π^* .

Next, we study pion valence DAs normalized to unity, or normalized pion valence DAs in vacuum and in medium. By this, we can study the change in shape due to the medium effects. We show in Fig. 5 the calculated normalized pion valence DAs, $\phi^*(x)$ both in vacuum ($\rho/\rho_0 = 0$) and in medium (left panel), and their magnifications (right panel). The in-medium change in shape is moderate when the nuclear densities are small, but it becomes evident when the density becomes ρ_0 .

Furthermore, it may be useful to define *effective pion valence DA* using the valence probability in vacuum η and in medium η^* . (See Eq. (16) and table 2.) The pion states in vacuum, $|\pi\rangle$, and in medium, $|\pi^*\rangle$, can respectively be

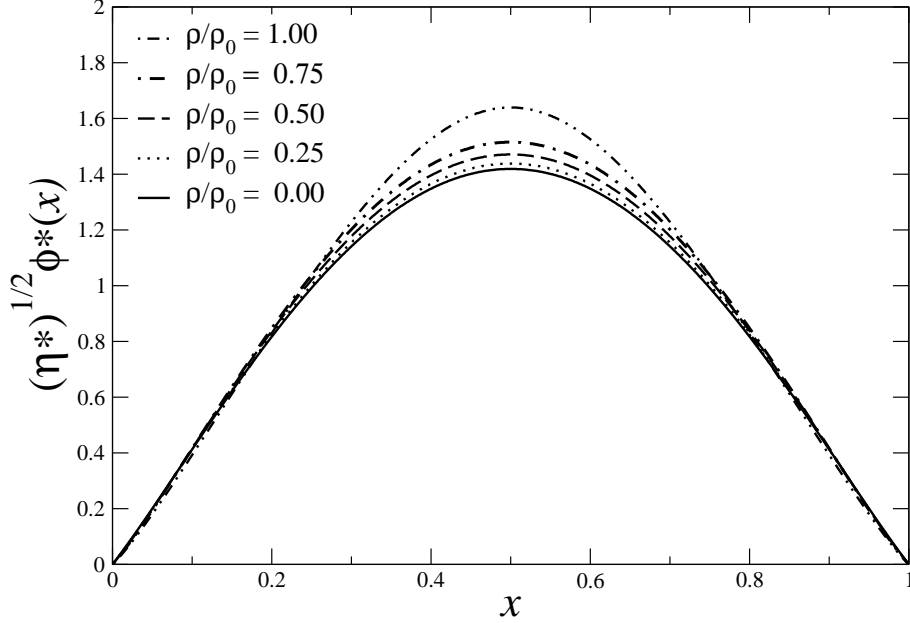


Fig. 6. Effective pion valence distribution amplitudes in vacuum and in medium, respectively multiplied by $\sqrt{\eta}$ and $\sqrt{\eta^*}$.

written as,

$$|\pi\rangle = \sqrt{\eta}|q\bar{q}\rangle + a|q\bar{q}q\bar{q}\rangle + b|q\bar{q}g\rangle + \dots, \quad (20)$$

$$|\pi\rangle^* = \sqrt{\eta^*}|q\bar{q}\rangle^* + c|q\bar{q}q\bar{q}\rangle^* + d|q\bar{q}g\rangle^* + \dots, \quad (21)$$

where a, b, c and d are constants, and g denotes a gluon, and $+\dots$ stands for the higher Fock components in the pion states. The quantity η^* in table 2 indicates that the valence $q\bar{q}$ component in the pion state increases in medium as nuclear density increases. The effective pion valence DAs, $\sqrt{\eta^*}\phi(x)^*$, in vacuum ($\rho/\rho_0 = 0$) and in medium are shown in Fig. 6. They may respectively correspond to the first terms of Eqs. (20) and (21).

Since η^*/η is enhanced in medium, effective pion valence DA in medium is also enhanced, on the top of the corresponding medium-(shape)modified normalized pion valence DA. The obvious enhancement of effective pion valence DA in medium can be seen around $x = 0.5$. This quantity may be useful when one studies some reactions in medium (in a nucleus) involving a pion, based on a constituent quark picture of pion.

Summary: We have studied the impact of in-medium effects on the pion valence distribution amplitudes using a light-front constituent quark model, combined with the in-medium input for the constituent light-quark properties calculated by the quark-meson coupling model. The in-medium constituent light-quark properties inside the pion are consistently constrained by the saturation prop-

erties of symmetric nuclear matter.

The in-medium pion mass is assumed to be the same as that in vacuum, based on the extracted information from the pionic-atom experiment, and some theoretical studies. This information extracted is valid up to around the normal nuclear matter density. Thus, the results obtained in this study, combined with the light-front constituent quark model, are valid up to around the normal nuclear matter density, but cannot discuss reliably the chiral limit, the vanishing limit of the (effective constituent) light-quark masses. We need to rely on more sophisticated models of pion to be able to discuss the chiral limit in medium, as well as in vacuum.

Due to the reduction in the pion decay constant in medium, the pion distribution amplitude in medium normalized with the pion decay constant, is appreciably reduced in nuclear medium. Because the valence component probability in medium increases as nuclear density increases, we have defined an effective pion distribution amplitude normalized to the square root of the valence probability in the pion state. This may give some information for the effectiveness of the valence quark picture of pion in nuclear medium. Within the present light-front constituent quark model approach, the effectiveness of the valence quark picture of the pion in medium, becomes more enhanced as nuclear density increases, due to the increase of the valence component in the pion state.

Although the present study is based on a simple, light-front constituent quark model, this is a first step to understand the impact of the medium effects on the internal structure of the pion immersed in nuclear medium. In the future, we plan to make similar studies for kaon, D-meson, and ρ -meson in nuclear medium.

Acknowledgements. This work was partly supported by the Fundação de Amparo à Pesquisa do Estado de São Paulo, Nos. 2015/17234-0, 2015/16295-5, 2016/04191-3 (FAPESP) and Conselho Nacional de Desenvolvimento Científico e Tecnológico, Nos. 400826/2014-3, 401322/2014-9, 308088/2015-8, 308025/2015-6 (CNPq) of Brazil.

References

- [1] G. E. Brown and M. Rho, Phys. Rev. Lett. **66**, 2720 (1991).
- [2] T. Hatsuda and S. H. Lee, Phys. Rev. C **46**, no. 1, R34 (1992).
- [3] For a review, K. Saito, K. Tsushima and A. W. Thomas, Prog. Part. Nucl. Phys. **58** (2007) 1.

- [4] For a review, R. S. Hayano and T. Hatsuda, *Rev. Mod. Phys.* **82**, 2949 (2010).
- [5] For a review, W. K. Brooks, S. Strauch and K. Tsushima, *J. Phys. Conf. Ser.* **299**, 012011 (2011).
- [6] J. P. B. C. de Melo, T. Frederico, L. Tomio and A. E. Dorokhov, *Nucl. Phys. A* **623** (1997) 456.
- [7] J. P. C. B. de Melo, H. W. L. Naus and T. Frederico, *Phys. Rev. C* **59** (1999) 2278.
- [8] J. P. B. C. de Melo, T. Frederico, E. Pace and G. Salmè, *Nucl. Phys. A* **707** (2002) 399.
- [9] J. P. B. C. de Melo, T. Frederico, E. Pace and G. Salme, *Braz. J. Phys.* **33**, 301 (2003).
- [10] E. O. da Silva, J. P. B. C. de Melo, B. El-Bennich and V. S. Filho, *Phys. Rev. C* **86** (2012) 038202.
- [11] G. H. S. Yabusaki, I. Ahmed, M. A. Paracha, J. P. B. C. de Melo and B. El-Bennich, *Phys. Rev. D* **92**(2015) 034017.
- [12] J. P. B. C. de Melo, I. Ahmed and K. Tsushima, *AIP Conf. Proc.* **1735**, 080012 (2016).
- [13] J. P. B. C. de Melo, K. Tsushima, B. El-Bennich, E. Rojas and T. Frederico, *Phys. Rev. C* **90** (2014) 035201.
- [14] J. P. B. C. de Melo, K. Tsushima and T. Frederico, *AIP Conf. Proc.* **1735**, 080006 (2016) doi:10.1063/1.4949459, [arXiv:1511.09219 [hep-ph]].
- [15] J. Fujita and H. Miyazawa, *Prog. Theor. Phys.* **17**, 360 (1957).
- [16] J. D. Sullivan, *Phys. Rev. D* **5**, 1732 (1972).
- [17] S. A. Coon, M. D. Scadron, P. C. McNamee, B. R. Barrett, D. W. E. Blatt and B. H. J. McKellar, *Nucl. Phys. A* **317**, 242 (1979).
- [18] M. Ericson and A. W. Thomas, *Phys. Lett. B* **128**, 112 (1983).
- [19] S. Weinberg, *Nucl. Phys. B* **363**, 3 (1991); *Phys. Lett. B* **295**, 114 (1992).
- [20] S. C. Pieper, V. R. Pandharipande, R. B. Wiringa and J. Carlson, *Phys. Rev. C* **64**, 014001 (2001).
- [21] T. Frederico, E. Pace, B. Pasquini and G. Salme, *Phys. Rev. D* **80**, 054021 (2009).
- [22] L. Adhikari, Y. Li, X. Zhao, P. Maris, J. P. Vary and A. Abd El-Hady, *Phys. Rev. C* **93**, no. 5, 055202 (2016).
- [23] C. Fanelli, E. Pace, G. Romanelli, G. Salme and M. Salmistraro, *Eur. Phys. J. C* **76**, no. 5, 253 (2016).

- [24] C. Mezrag, L. Chang, H. Moutarde, C. D. Roberts, J. Rodriguez-Quintero, F. Sabati and S. M. Schmidt, *Phys. Lett. B* **741**, 190 (2015).
- [25] C. Chen, L. Chang, C. D. Roberts, S. Wan and H. S. Zong, *Phys. Rev. D* **93**, 074021 (2016).
- [26] P. T. P. Hutaauruk, I. C. Cloet and A. W. Thomas, *Phys. Rev. C* **94**, 035201 (2016).
- [27] M. Ericson and A. W. Thomas, *Phys. Lett. B* **128**, 112 (1983).
- [28] S. A. Kulagin, *Nucl. Phys. A* **500**, 653 (1989).
- [29] K. Suzuki, *Phys. Lett. B* **368**, 1 (1996).
- [30] P. A. M. Guichon, *Phys. Lett. B* **200**, 235 (1988).
- [31] P. A. M. Guichon, K. Saito, E. N. Rodionov and A. W. Thomas, *Nucl. Phys. A* **601** (1996) 349;
K. Saito, K. Tsushima and A. W. Thomas, *Nucl. Phys. A* **609**, 339 (1996);
Phys. Rev. C **55**, 2637 (1997);
K. Tsushima, K. Saito, J. Haidenbauer and A. W. Thomas, *Nucl. Phys. A* **630**, 691 (1998);
P. A. M. Guichon, A. W. Thomas and K. Tsushima, *Nucl. Phys. A* **814** (2008) 66.
- [32] B. D. Serot and J. D. Walecka, *Adv. Nucl. Phys.* **16**, 1 (1986).
- [33] J. R. Stone, N. J. Stone and S. A. Moszkowski, *Phys. Rev. C* **89**, 044316 (2014).
- [34] For a review, see P. Kienle and T. Yamazaki, *Prog. Part. Nucl. Phys.* **52**, 85 (2004).
- [35] U. G. Meissner, J. A. Oller and A. Wirzba, *Annals Phys.* **297**, 27 (2002).
- [36] U. Vogl and W. Weise, *Prog. Part. Nucl. Phys.* **27**, 195 (1991).
- [37] H. M. Choi and C. R. Ji, *Phys. Rev. D* **75**, 034019 (2007).
- [38] T. Huang, T. Zhong and X. G. Wu, *Phys. Rev. D* **88**, 034013 (2013).
- [39] Seung-il Nam and C. W. Kao, *Phys. Rev. D* **85**, 094023 (2012).
- [40] Seung-il Nam, *Phys. Rev. D* **86** (2012) 074005.
- [41] B. El-Bennich, J. P. B. C. de Melo, B. Loiseau, J.-P. Dedonder and T. Frederico, *Braz. J. Phys.* **38** (2008) 465.
- [42] R. Van Royen and V. F. Weisskopf, *Nuovo Cim. A* **50**, 617 (1967) Erratum: [*Nuovo Cim. A* **51**, 583 (1967)].
- [43] S. V. Mikhailov and A. V. Radyushkin, *JETP Lett.* **43** (1986) 712 [*Pisma Zh. Eksp. Teor. Fiz.* **43** (1986) 551].
- [44] A. P. Bakulev, S. V. Mikhailov and N. G. Stefanis, *Phys. Lett. B* **508** (2001) 279, Erratum: [*Phys. Lett. B* **590** (2004) 309].

- [45] S. Dalley, Phys. Rev. D **64** (2001) 036006.
- [46] G. P. Lepage, S. J. Brodsky, T. Huang and P. B. Mackenzie, CLNS-82-522, FERMILAB-CONF-81-114-T.
- [47] S. J. Brodsky and G. P. Lepage, Adv. Ser. Direct. High Energy Phys. **5**, 93 (1989).